BGSG

Volume 58

Research Paper

NEOGENE-QUATERNARY TECTONIC REGIME AND MACROSEISMIC OBSERVATIONS IN THE TYRNAVOS-ELASSONA BROADER EPICENTRAL AREA OF THE MARCH 2021, INTENSE EARTHQUAKE SEQUENCE

Dimitrios Galanakis [1], Sotiris Sboras [1,2], Garyfallia Konstantopoulou [1], Markos Xenakis [1]

[1]Hellenic Survey of Geological and Mineral Exploration (HSGME), Sp. Loui 1, GR136 77, Acharnae, galanakis@igme.gr kongar@igme.gr markxen@igme.gr

[2]Institute of Geodynamics, National Observatory of Athens, Lofos Nymfon, Thission, GR118 10, Athens ssboras@gmail.com

Correspondence to:
Dimitrios Galanakis
galanakis@igme.gr

DOI number:
http://dx.doi.org/10.12681/bgsg.27196

Keywords:
2021 Tyrnavos-Elassona earthquake, macroseismic observations, ground deformation phenomena, seismotectonics

Citation:
Galanakis, D., Sboras, S., Konstantopoulou, G. and Xenakis, M. (2021), Neogene-Quaternary Tectonic Regime and Macroseismic Observations in The Tyrnavos-Elassona Broader Epicentral Area of The March 2021, Intense Earthquake Sequence. Bulletin Geological Society of Greece, 58, 200-221.

Publication History:
Received: 04/06/2021
Accepted: 23/09/2021
Accepted article online: 24/09/2021

The Editor wishes to thank Christoph Gruetzner and Haralambos Kranis for their work with the scientific reviewing of the manuscript and Ms Emmanouela Konstantakopoulou for editorial assistance.

Abstract

On March 3, 2021, a strong (Mw6.3) earthquake occurred near the towns of Tyrnavos and Elassona. One day later (March 4), a second strong (Mw6.0) earthquake occurred just a few kilometres toward the WNW. The aftershock spatial distribution and the focal mechanisms revealed NW-SE-striking normal faulting. The focal mechanisms also revealed a NE-SW oriented extensional stress field, different from the orientation we knew so far (ca. N-S). The magnitude and location of the two strongest shocks, and the spatiotemporal evolution of the sequence, strongly suggest that two adjacent fault segments were ruptured respectively. The sequence was followed by several coseismic ground deformational phenomena, such as landslides/rockfalls, liquefaction and ruptures. The landslides and rockfalls were mostly associated with the ground shaking. The ruptures were observed west of the Titarissios River, near to the Quaternary faults found by bore-hole lignite investigation. In the same direction, a fault scarp separating the alpidic basement from the alluvial deposits of the Titarissios valley implies the occurrence of a well-developed fault system. Some of the ground ruptures were accompanied by extensive liquefaction phenomena. Others cross-cut reinforced concrete irrigation channels without changing their direction. We suggest that this fault system was partially reactivated, as a secondary surface rupture, during the sequence as a steeper splay of a deeper low-to-moderate angle normal fault.

Περίληψη

Στις 3 Μαρτίου 2021 ισχυρός (M_w=6.3) σεισμός καταγράφηκε κοντά στις πόλεις του Τυρνάβου και της Ελασσόνας. Την επόμενη ημέρα, δεύτερος ισχυρός (M_w=6.0) σεισμός χτύπησε την περιοχή, μόλις λίγα χιλιόμετρα προς τα ΔΒΔ. Η χωρική κατανομή της μετασεισμικής ακολουθίας και οι μηχανισμοί γένεσης αποκάλυψαν την ύπαρξη κανονικούς ρήγματος παράταξης ΒΔ-ΝΑ. Οι μηχανισμοί γένεσης επίσης αποκάλυψαν ένα εφελκυστικό πεδίο προσανατολισμού ΒΑ-ΝΔ, διαφορετικού απ' αυτόν που γνωρίζαμε μέχρι πρότινος (περίπου Β-Ν). Το μέγεθος και η επικεντρική θέση των δύο ισχυρών σεισμών, καθώς και η χωρο-χρονική εξέλιξη της ακολουθίας, υποστηρίζουν σθεναρά την διάρρηξη δύο διπλανών ρηξιγενών τμημάτων αντίστοιχα. Η ακολουθία συνοδεύτηκε από αρκετά φαινόμενα συν-σεισμικής εδαφικής παραμόρφωσης, όπως κατολισθήσεις/βραχοπτώσεις, ρευστοποιήσεις και εδαφικές διαρρήξεις. Οι κατολισθήσεις και βραχοπτώσεις συνδέονται κυρίως με την εδαφική κίνηση. Οι διαρρήξεις εντοπίστηκαν δυτικά του ποταμού Τιταρήσιος, πολύ κοντά σε Τεταρτογενή ρήγματα που ανακαλύφθηκαν παλαιότερα από τη διάνοιξη συστήματος γεωτρήσεων κατά την έρευνα για λιγνιτικά κοιτάσματα. Στην ίδια διεύθυνση, ένα τεκτονικό πρανές που χωρίζει το αλπικό υπόβαθρο από τις αλλουβιακές αποθέσεις της κοιλάδας του Τιταρήσιου υποδεικνύουν την ύπαρξη ενός καλά ανεπτυγμένου συστήματος ρηγμάτων. Αρκετές από τις εδαφικές διαρρήξεις συνδέονταν με φαινόμενα ρευστοποίησης. Κάποιες άλλες διέρρηξαν αρδευτικά κανάλια από οπλισμένο σκυρόδεμα χωρίς να αλλάξουν διεύθυνση. Προτείνεται ότι αυτό το σύστημα ρηγμάτων συμμετείχε μερικώς στη διάρρηξη των σεισμών του 2021 ως ένας κλάδος ενός βαθύτερου κανονικού ρήγματος μέσης έως μικρής γωνίας κλίσης.

Keywords: *2021 Tyrnavos-Elassona earthquake, macroseismic observations, ground deformation phenomena, seismotectonics*

1. INTRODUCTION

On March 3, 2021, at 10:16 UTC, a strong earthquake (M_w=6.3) occurred in northern Thessaly. One day later (March 4, 18:38 UTC), a second strong shock (M_w=6.0) occurred few kilometres WNW of the first one. Until the end of March, five (5) earthquakes greater than M_L=5.0 occurred in the epicentral area. Surprisingly, the focal mechanisms of the strongest shocks did not show E-W striking like we used to know as a typical direction of the active faults of Thessaly (*e.g.*, Caputo, 1993; Caputo and Pavlides, 1993; Caputo *et al.*, 2012); they revealed NW-SE-striking, pure normal dip-

slip faulting, in a NE-SW oriented extensional field. In fact, a NE-SW oriented field was proposed for the previous tectonic phase that characterized broader Thessaly, *i.e.*, during Pliocene and Early Pleistocene (Caputo and Pavlides, 1991; 1993).

The affected area is located west of Mt Antichasia, east of Mt Trochalos and Mt Papalivado, which constitute the natural boundary from the Elassona sub-basin, and north of Mt Zarkos (Fig. 1). The stricken settlements are Domeniko, Magoula, Amourio, Evangelismos, Praitorio, Mesochori and Damasi, all situated in "Domeniko-Amourio" area. The ca. N-S-trending Neogene tectonic basin of Domeniko-Amourio (broader Elassona) is crossed by the Elassonitikos River, and further eastwards it enters the E-W-trending tectonic valley of Titarissios River. The Domeniko-Amourio Basin and the Titarissios valley are both intra-montane landforms, surrounded by the aforementioned mountains. The basins show a rather smooth terrain, at the margins of which most of the settlements are located, while the mountainous area is quite ragged considering that it consists of Mesozoic marbles and Paleozoic gneiss-schists (IGME, 1987; 1998). Drainage is dense and the main rivers are supplied by small and large torrents of continuous or seasonal flow. It is locally controlled by faults.

2. GEOLOGICAL SETTING

The Elassona Basin comprises the southern part of a larger depression starting from Florina to the north, and it is known for the rich in lignite-bearing sediments. It consists of two sub-basins: the northeastern one where the town of Elassona is situated, and the southwestern one, the Domeniko-Amourio sub-basin, where the epicentral area lies. These two sub-basins are connected through the Agioneri pass and the Elassonitikos valley. They both belong to the Pelagonian zone. The mountainous area is occupied by the alpidic basement (Fig. 1). The Neopalaeozoic – Lower-Middle Triassic schist-crystalline rocks occupy the SW and N part of the area and they are composed of gneisses and schist-gneiss with marble intercalations (lower members), and (bi)micaceous schists, quartzite, and orthogneiss. Granite and granodiorite intrusions occur in the schist-crystalline rocks that took place before the Pelagonian thrust. The schist-crystalline rocks pass into crystalline limestone of Triassic – Jurassic age. All the above formations of the Pelagonian zone are obducted upon an autochthonous thick series of marbles (Neopalaeozoic – Jurassic age). This series outcrops as a tectonic window at the NW part of the area. The alpidic presence is completed with the ophiolites.

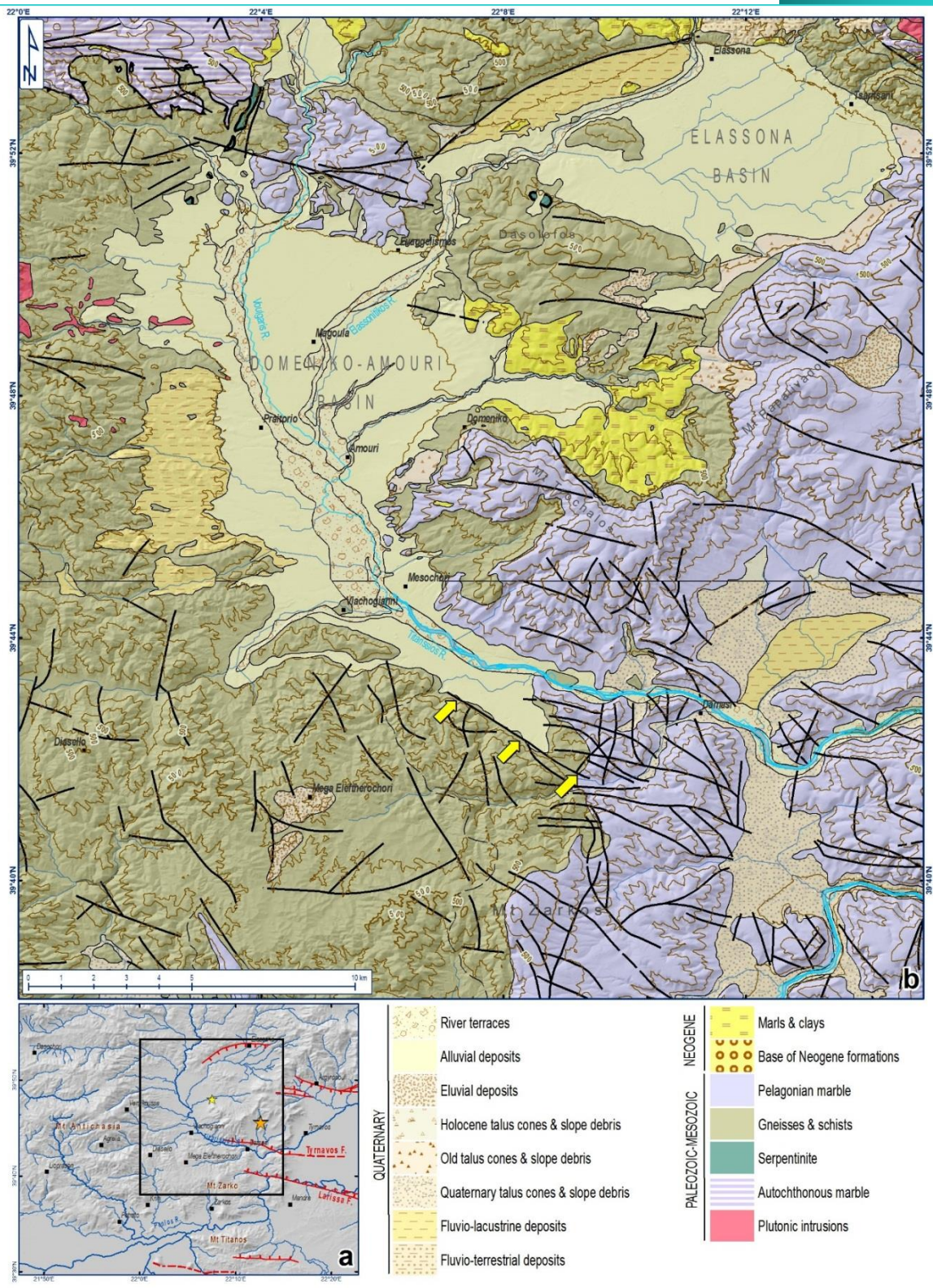

Fig. 1: Simplified geological map of the 2021 Tyrnavos-Elassona epicentral area (modified after IGME, 1987; 1998). Yellow arrows point to a fault we suggest that it partially participated in the 2021 sequence.

The neotectonic, palaeoclimatic and palaeogeographic conditions combined, facilitated the basin's formation and its fill with younger sediments. Thus, the basin is filled with Neogene and Quaternary deposits in which significant lignitic deposits are found. The Neogene (Pliocene) formations are unconformably deposited upon the schist-crystalline basement, they are significantly developed, and they mostly outcrop along the margins of Domeniko-Amourio sub-basin. In more detail, they occupy the hills at the eastern part of the sub-basin. They consist of light-coloured marl, clay and platy marly limestone with very shallow dip. In the steeper valleys, the red series of the Neogene base is observed made of sandstone and clay. The lignite-bearing layers are included in the whitish marl. The most recent deposits that overly the Neogene ones are alluvial deposits of sand, clay and unconsolidated rounded and angular gravel, river terraces, talus cones, slope debris, and deposits lying along river and torrent banks.

The slope gradient map (Fig. 2), which is based on the AW3D30 (ALOS World 3D – 30 m; Tadono *et al.*, 2014)) elevation grid, shows interesting morphological characteristics depending on the geological formations and tectonics (Fig.1). The post-alpidic sediments show a mild/smooth relief with values rarely exceeding 12° (*e.g.*, the fluvio-lacustrine deposits west of Praitorio and west of Elassona). The roughest relief belongs to the marble. Faulting has the strongest impact on the relief by forming linear steep slopes (>18°). Two characteristic examples are the several kilometres-long, ENE-WSW- to NE-SW-trending mountain-front west of Elassona, and the NW-SE-trending linear slope bounding the southern margin of the Titarissios valley. The latter has been also recognised in the 1:50,000 scale geological map ("Farkadon" sheet) of IGME (1998) (marked by yellow arrows in Fig. 1). There are also some other linear slopes, along the southeastern margin of the Elassona Basin and the southwestern margin of the Domeniko-Amourio sub-basin, which are not related to any faulting according to the literature. It is, though, an indication, but not proof, of possible (normal) fault occurrences.

During the mine research in the area by IGME (Dimitriou and Giakoupis, 1998), a dense network of boreholes was drilled revealing important tectono-stratigraphic information for the Domeniko-Amourio sub-basin (Fig. 3). Stratigraphically, the post-alpidic formations found within the basin consist of (from older to younger; Fig. 3c): i) conglomerates and clay-sandy deposits, mostly of fluvio-torrential origin, ii) the lignite-bearing formation of Upper Miocene – Pliocene, composed at its base by mud, sandy clayey and sands with thin lenses of granules and thin interbeds of pure mud, in which the lignitic deposits occur in the form of lenses and intercalations, and at its upper members by friable and rarely stiff marls alternated with clay-marly material and

interbeds of marly limestone, and iii) fluviolacustrine and fluvio-torrential Quaternary deposits composed by clay-sandy materials (sandstones, clays and fine-grained conglomerates), alluvial deposits of sands, as well as river terraces, talus cones and slope debris.

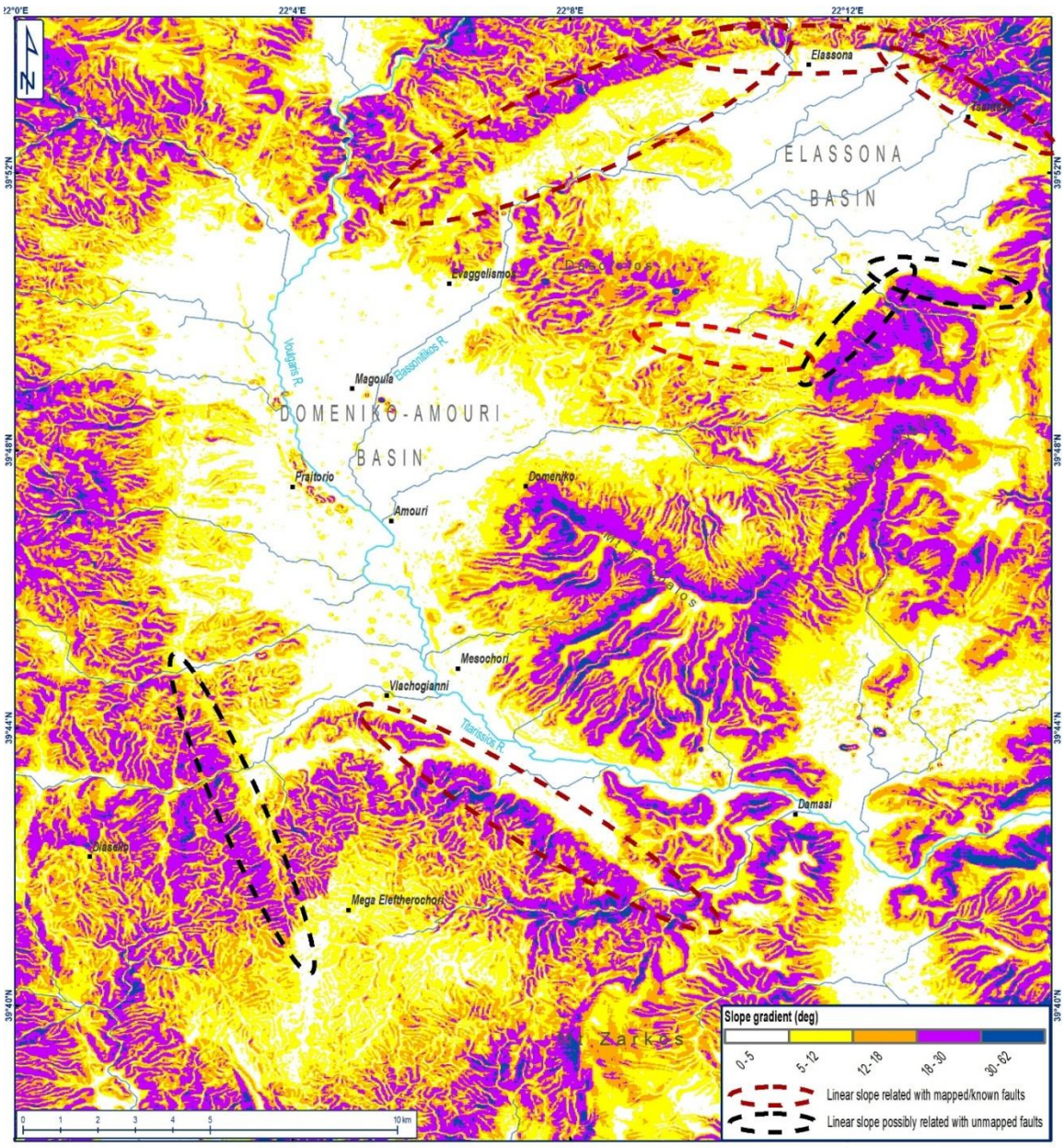

Fig. 2: Slope gradient map of the broader 2021 epicentral area based on the AW3D30 (ALOS World 3D – 30 m; Tadono *et al.*, 2014) elevation grid. The dashed ellipses mark linear slopes of mapped (or known) faults (dark red) or linear slopes implying the occurrence of normal faults (black).

3. GEODYNAMIC AND SEISMOTECTONIC SETTING

The geodynamic regime of the broader study area was under an extensional stress field of NE-SW orientation during Pliocene – Early Pleistocene and created the major faults that formed the tectonic basins of Thessaly in a NW-SE direction. During the Quaternary, the extensional stress field changed direction into N-S which is supposed to be the active one today and which formed the ca. E-W-striking normal faults (*e.g.*, Caputo and Pavlides, 1993). Based on the tectonostratigraphic interpretation of the Domeniko-Amourio sub-basin in the technical report of the lignite-deposits investigation (Dimitriou and Giakoupis, 1998), besides the topmost Holocene deposits, the rest formations that fill the sub-basin are often observed vertically displaced from borehole to borehole, implying the occurrence of normal dip-slip faulting (Fig. 3b, d). All implied faults are not of the same age since they either displace the deeper Upper Miocene formations, or they displace the base of Quaternary (Villafranchian). The younger faults, characterized as 'post-Neogene' faults, demonstrate a NW-SE direction forming bookshelf or graben-style patterns (Fig. 3b, d). Along the SW margin of Domeniko-Amourio sub-basin, a fault of similar direction, dipping to the NE, created a downthrow of several tens of metres (fault f11; Fig. 3). This fault lies in the extension of the coseismic ground ruptures and the liquefaction phenomena which were mapped south of the Titarissios river.

Historic and early instrumental records of earthquakes (*e.g.*, Papazachos and Papazachou, 2003) reveal the occurrence of few strong ($M \geq 6.0$) events in north-eastern Thessaly (Fig. 4b). Although the location and magnitude estimations are of low accuracy for old events, the proposed epicentres are mostly located in the east Thessalian Basin. In the 20th c. only one notable event of $M \geq 6.0$ occurred in this area, the magnitude of which is explicitly discussed by Caputo and Helly (2005). The recent seismic activity of the last 10 years, prior to the March 3, 2021 earthquake, reveals a cluster in the narrow epicentral area of maximum M_L=3.6 (Fig. 4c). During this period, in 2013 the cluster completely lacks any event, while in 2011, 2014 and 2017 just a few events ($M < 5$) were recorded. The surrounding area is quite poor in events, especially the biggest part of the East Thessalian Basin.

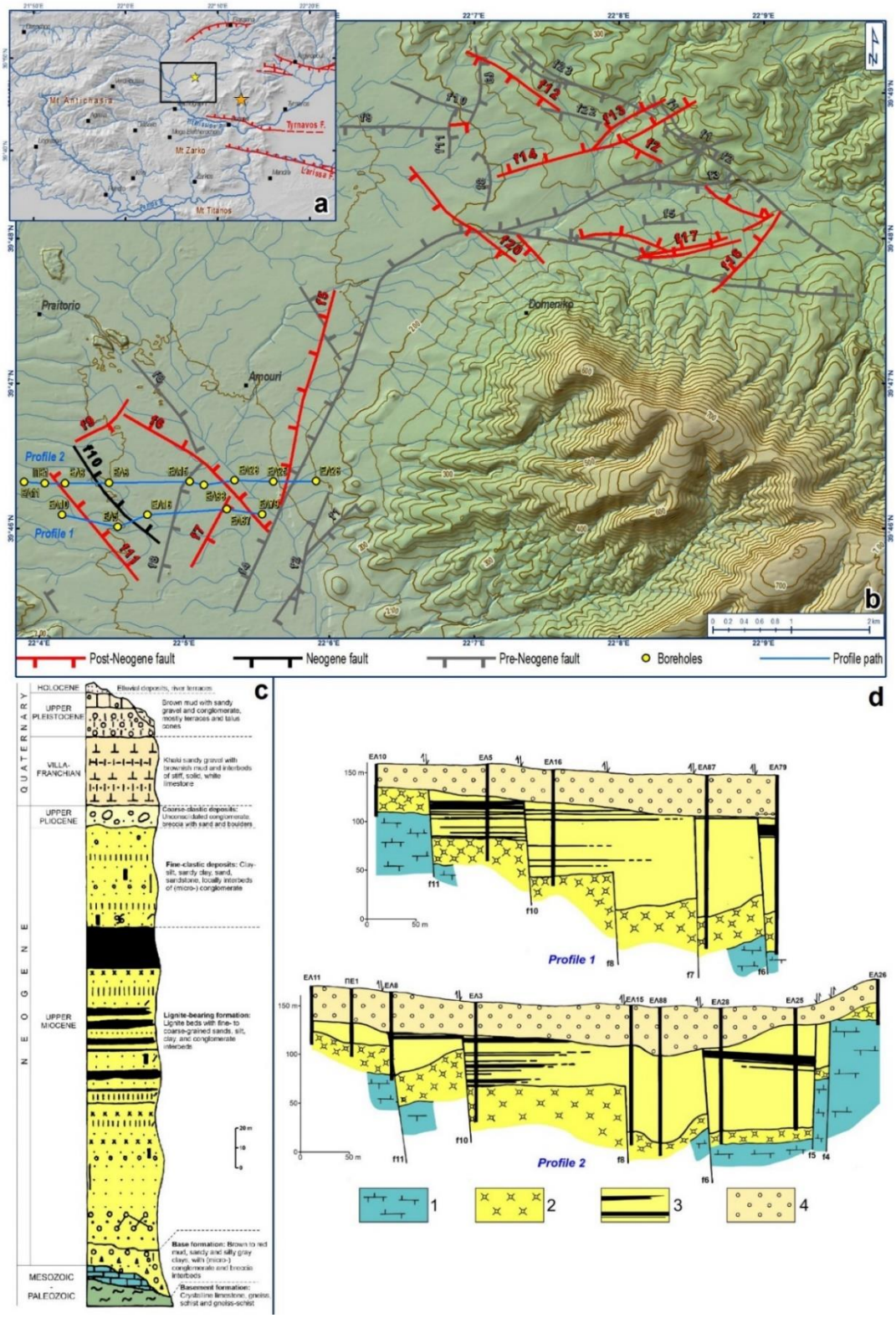

Fig. 3: a) Hillshade map of the broader 2021 epicentral area showing the epicentres of the strongest shocks (orange star = March 3, Mw=6.3, yellow star = March 4, Mw=6.0), and the neotectonic faults according to literature (for references see main text). b) Shaded relief map exported from the 5 m-DEM of Hellenic Cadastre where the fault locations suggested by IGME's study are shown (after Dimitriou and Giakoupis, 1998). The location of selected boreholes and the profile paths of inset (d) are also shown. c) Synthetic stratigraphic column of the Neogene formations of the Elassona Basin, according to the above study (after Dimitriou and Giakoupis, 1998, modified). d) Interpreted profiles based on borehole data according to Dimitriou and Giakoupis

(1998). Lithology is simplified: 1 = alpidic basement, 2 = base formation (Upper Miocene), 3 = lignite-bearing formation with the fine- and coarse-clastic deposits (Upper Miocene - Villafranchian), 4 = Quaternary deposits (Upper Pleistocene – Holocene).

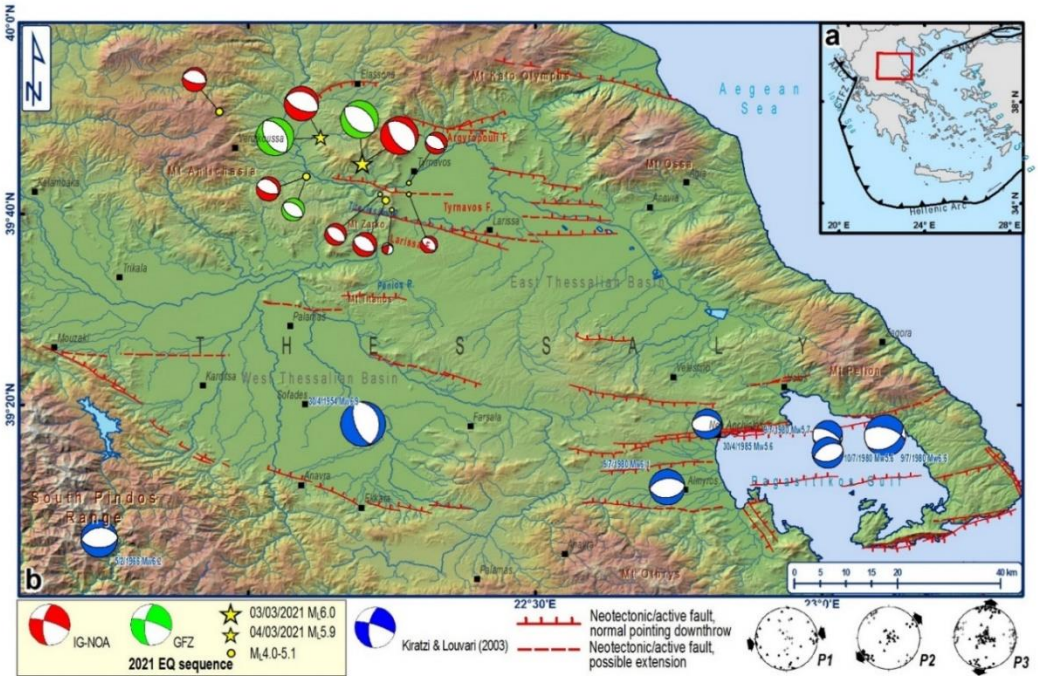

Fig. 4: (a) Map of the Aegean region showing the major crustal-scale tectonic structures (AACZ = Apulian-Aegean Collision Zone; CTFZ = Cephalonia Transform Fault Zone; NAT = North Aegean Trough) and the location of map (b). (b) Shaded relief map of Thessaly showing the major neotectonic/active faults (after Galanakis, 1997; Caputo and Pavlides, 1991; 1993; Perissoratis *et al.*, 1991; Sboras, 2011; Caputo *et al.*, 2012; GreDaSS), focal mechanisms of past significant events (Kiratzi and Louvari, 2003) and the focal mechanisms calculated by IG-NOA and GFZ for the strongest shocks of the 2021 earthquake sequence near Tyrnavos. P1, P2 and P3 (bottom right corner) are the three last tectonic phases after a meso-structural analysis in Thessaly (Caputo and Pavlides, 1993) revealing ca. E-W compression during early to middle Miocene (*P1*), NE-SW extension during Pliocene – Early Pleistocene (*P2*), and ca. N-S extension from middle Pleistocene to Today (*P3*).

4. THE MARCH 2021 SEISMIC SEQUENCE

The March 2021 sequence changed our view of what was so far known about the direction of both active faults and the extensional axis. The published moment tensor solutions revealed NW-SE-striking, almost pure normal dip-slip faulting, and consequently a NE-SW oriented extensional axis (Fig. 4b). The sequence evolved in the uppermost 25 km of the crust and was constrained west of the Tyrnavos Basin (East Thessalian Basin). The mainshock (M_W6.3) is located in the mountainous area north of Titarissios River. The second strongest shock (M_W6.0) occurred ca. 8.5 km WNW of

the mainshock. The spatiotemporal evolution of the sequence (Fig. 5) shows that the strongest aftershock occurred near the north-western edge of the epicentral distribution until that time. After the M_W6.0 event, the sequence started to develop further to the WNW (Fig. 5b, c). In Fig. 5c (8 days period after the M_W6.0 event), the WNW part of the sequence was denser than the ESE one and seems to have a slight change of trend direction (towards NW-SE). Seeing all events from day 1 (March 3) until March 31 (Fig. 5d), the sequence is developed along a distance of ca. 42 km with a WNW-ESE trend. The distance between the M_W6.0 event and the WNW edge of the sequence is more than 20 km. From the preliminary seismological data, it seems that two (adjacent) fault segments were activated during the March 2021 sequence.

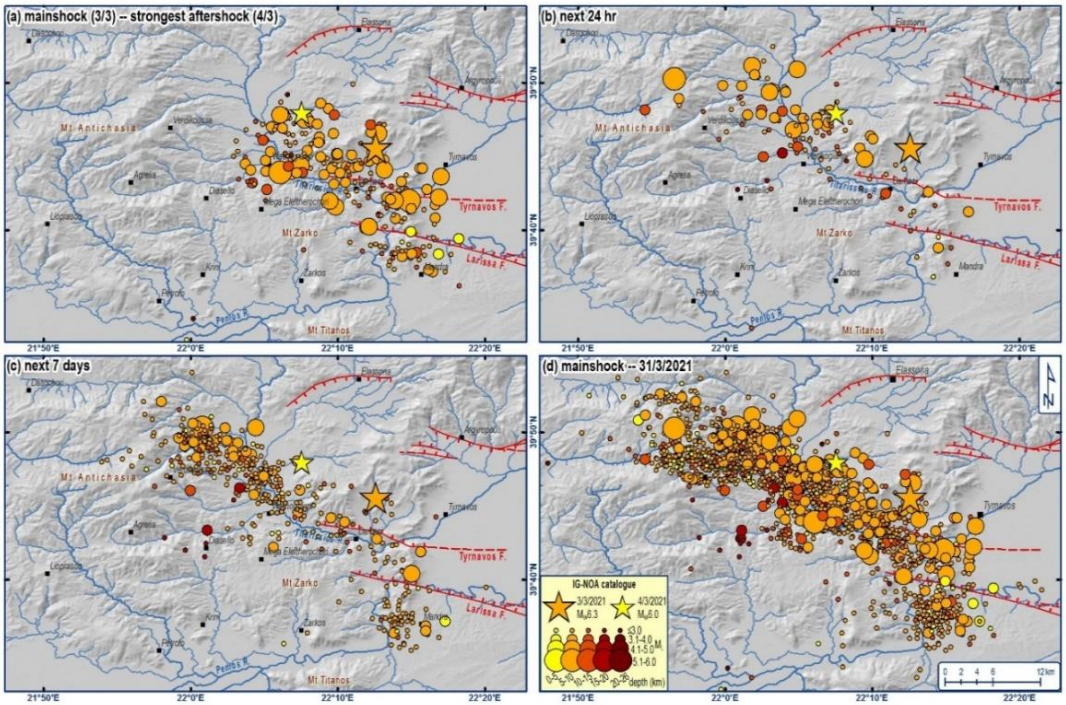

Fig. 5: Spatiotemporal evolution of the March 2021 seismic sequence in northern Thessaly: a) from the mainshock to the strongest aftershock (March 4), b) 24 hr after the strongest aftershock (March 4), c) 7 days after (c), and d) all events from the mainshock to the end of March. Epicentres obtained from the IG-NOA catalogue (http://www.gein.noa.gr/en/seismicity/earthquake-catalogs) .

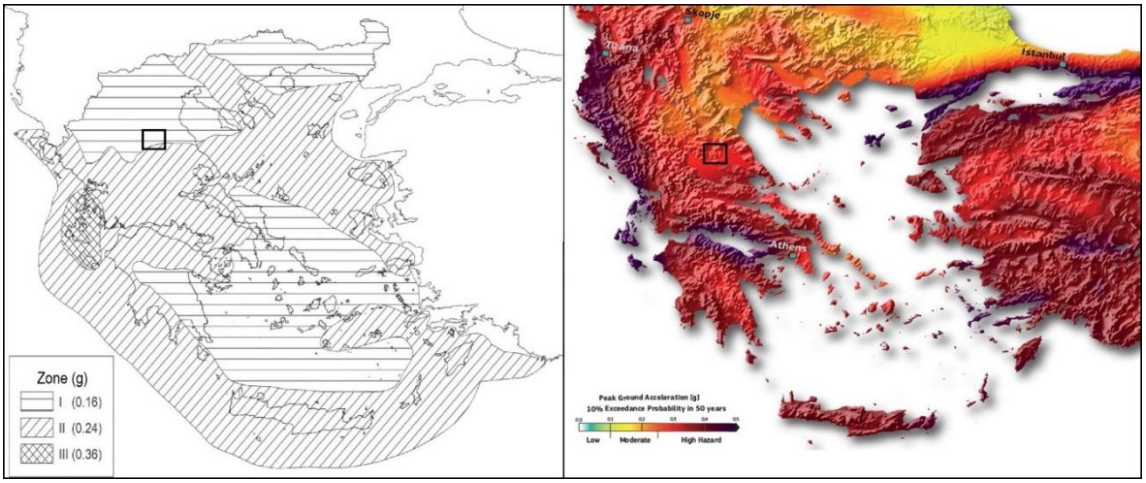

Fig. 6: *(Left)* The EPPO (2000) seismic hazard map of Greece. *(Right)* The SHARE seismic hazard map (Giardini *et al.*, 2014; Woessner *et al.*, 2015). The study area is marked by a black rectangular.

5. THE MARCH 2021 COSEISMIC (GROUND) EFFECTS

The intense earthquake activity of the March 2021 sequence caused one death, three light injuries, and heavy damages with more than 1700 buildings (houses, schools, churches, etc.) beyond repair. According to the Greek Antiseismic Regulation (EPPO, 2000) and the modified seismic hazard map (Fig. 6; Greek Government Gazette 1154B/12.8.2003), the broader Tyrnavos-Elassona region belongs to Seismic Risk Zone II (planning ground acceleration 0.24 g). The hazard map of the SHARE European project (Fig. 6; Giardini *et al.*, 2014; Woessner *et al.*, 2015) suggests 0.23 g < PGA < 0.29 g for the broader epicentral area. According to the preliminary report by the Institute of Engineering Seismology and Earthquake Engineering (ITSAK-DUTh, 2021; Fig. 7), the PGA recorded value in Larissa City is approx. 140 cm/s^2.

The seismic crisis was accompanied with several co-seismic ground deformational effects, such as secondary ground ruptures, rockfalls and liquefaction (Fig. 8; Fig. 9).

5.1. Landslides and Rockfalls

Along the Tyrnavos-Elassona highway, a 9 km-long part of the road is opened in the Mesozoic marble along the eastern mountain-front where rockfalls occurred (Fig. 9e). The artificial slope (sometimes along both sides of the road) is steep and locally significantly high, and the marble which it is made of is severely fractured, forming

suitable conditions for the detachment of multi-sized rock-blocks (slide/wedging/capsizing).

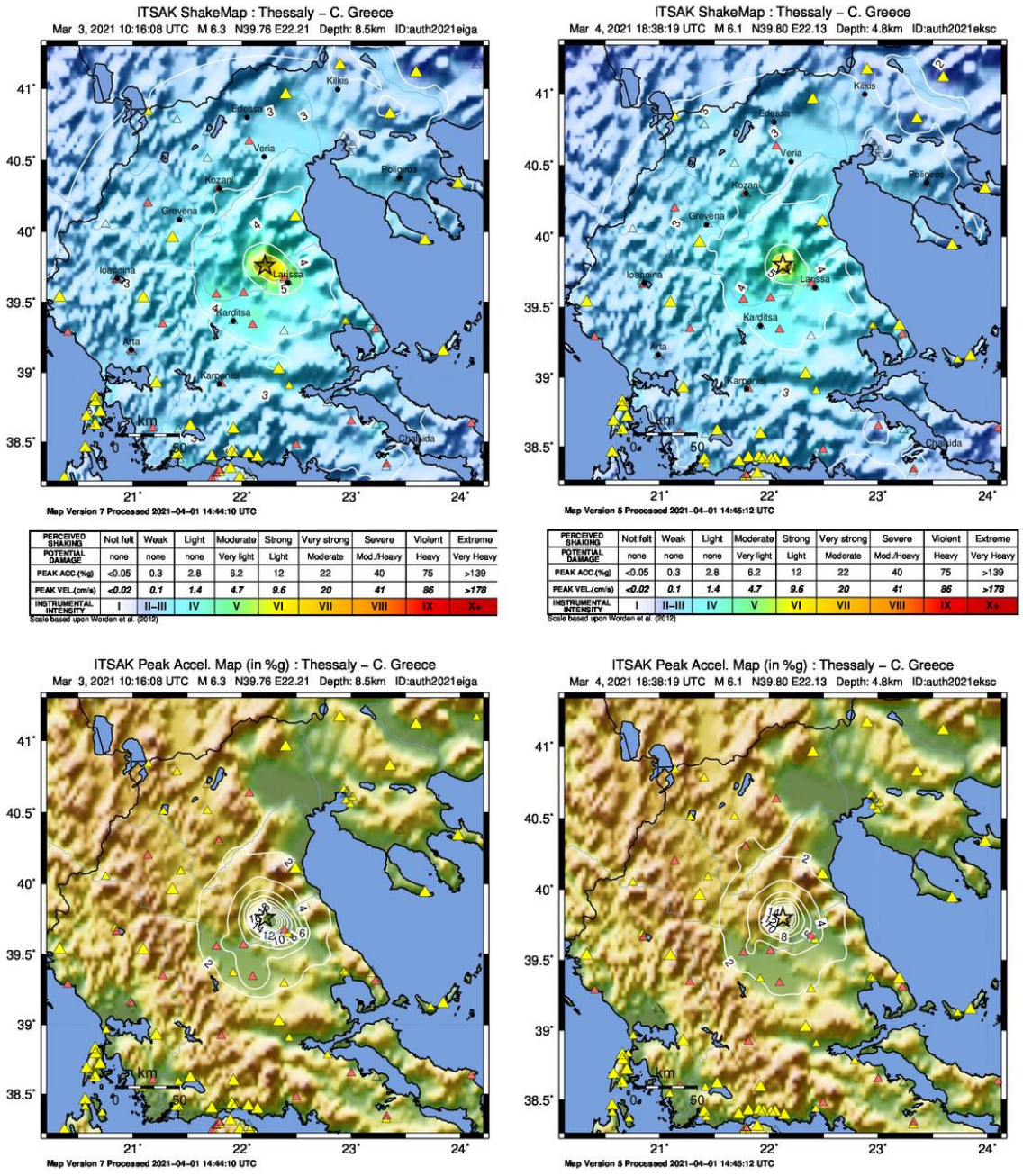

Fig. 7: Shakemaps (*Top*) and PGA maps (*Bottom*) of the March 3 (*Left*) and March 4 (*Right*) strong shocks, by the Institute of Engineering Seismology and Earthquake Engineering (ITSAK).

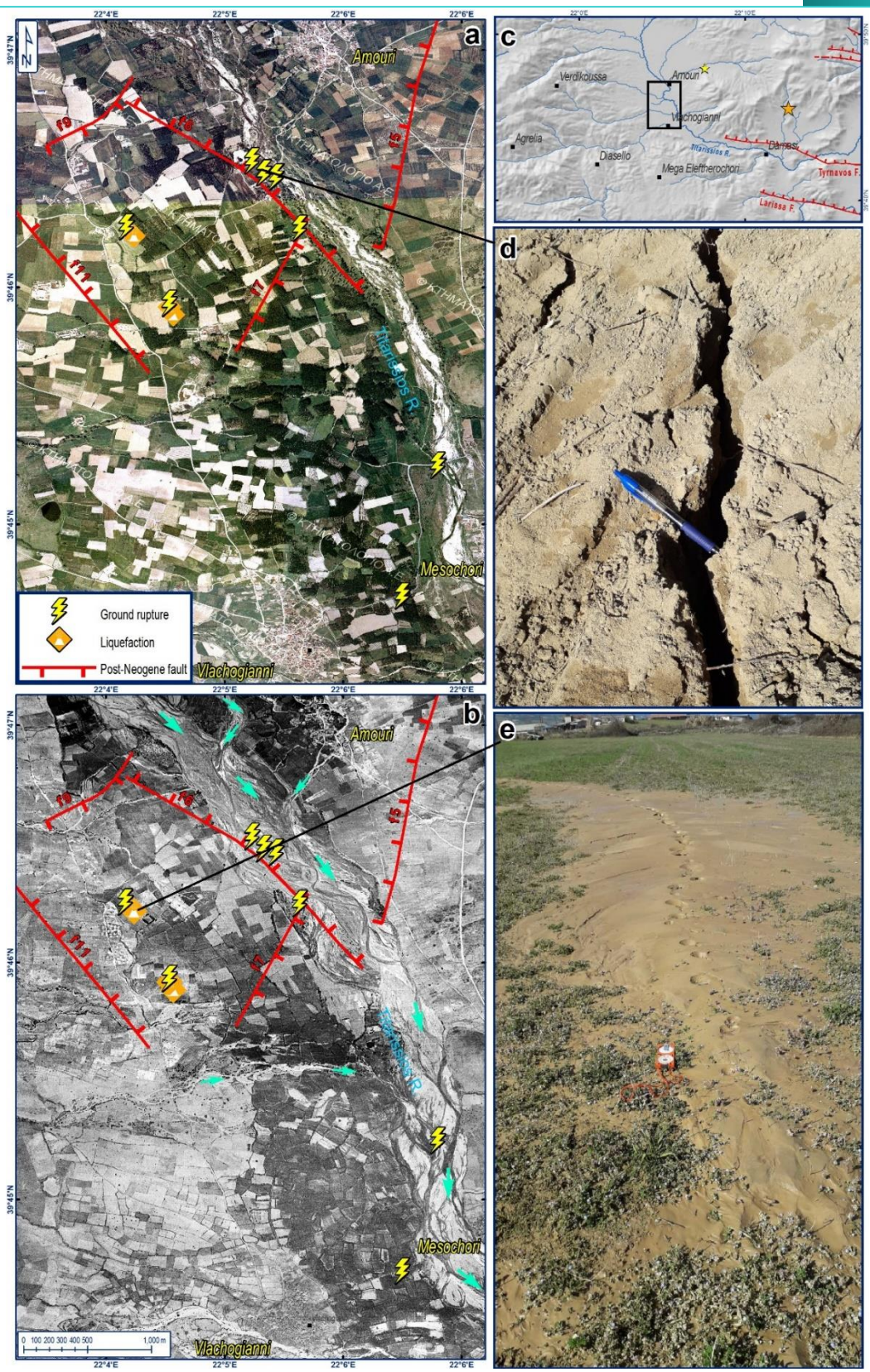

Fig. 8: Photomosaic (a, b) of the epicentral area where ground deformation phenomena were observed. The 'post-Neogene' faults of IGME's study (Dimitriou and Giakoupis, 1998) are also shown. In (b), the flow direction of the Elassonitis-Titarissios river and its tributaries is marked with light-blue arrows. Both photomosaics are obtained from the Hellenic Cadastre, dated in 2016 (a) and 1945-1946 (b); their location is shown on the hillshade map (c). Co-seismic ground ruptures (d, e), also associated with liquefaction (e). The general trend of the ruptures is NW-SE.

On the local road towards the Panagia Olympiotissa Monastery (Elassona), at the inner slope below the monastery, rockfalls of various sizes were recorded (Fig. 9g, h). The hill consists of semi-cohesive materials of a river terrace. The coarse-grained material includes rounded boulders of various sizes, rounded and angular gravel, whilst the fine-grained material is mostly sand; the matrix is of calcareous composition. Due to the progressive erosion of the fine-grained material, loose and unstable boulders are formed along the slope front, susceptible to falling after heavy rain or seismic ground shaking.

Next to the Agioi Anargyri church, in Domeniko village, the seismic ground shaking caused the detachment of a gneiss-schist boulder (ca. 5 m^3 volume), shifted only for 20-40 cm (Fig. 9d). The detachment was probably facilitated by the occurrence of a pre-existing fissure, along the length of which a root system of an adjacent tree was developed.

5.2. Ground Ruptures

In the broader area among the villages Mesochori, Vlachogianni, Varko, Praitorio and Amourio, the rivers Elassonitikos and Titarissios converge making the total thickness of the alluvial deposits and Pleistocene sediments exceed 70 m in thickness, which along with the high hydrological conditions, facilitate liquefaction phenomena and ground ruptures. It is noteworthy that the ground ruptures formed near and parallel to the Neogene and 'post-Neogene' faults discovered by Dimitriou and Giakoupis (1998), implying that the ruptures also prefer to follow older tectonic discontinuities as well. Several ground ruptures were observed, many times with liquefaction phenomena, along two main linear layouts: the eastern one, near the Titarissios River, has a total extent of *ca.* 3.5 km and the western one is at least 2.5 km long totally. These deformational effects were traced in farmed fields or they were crossing the road network, forming a NW-SE-striking zone, parallel to the Titarissios River and the nodal planes proposed by the focal mechanisms (Fig. 4). The ground ruptures outcrop as S-shaped extensional fissures, with a heave ranging from few millimetres up to 10 cm (locally even wider).

It is noteworthy that the ground ruptures did not stop on constructions. In two cases along the local irrigation channel network, which is made of reinforced concrete, the ruptures crossed the channels regardless of their direction (Fig. 10). In Fig. 10c, where the channel's direction is sub-parallel to the ruptures, the fissures on the reinforced concrete only slightly diverted their direction, although the easiest way was to break the construction quasi-perpendicularly. The aligned pattern parallel to the blind faults of

Dimitriou and Giakoupis (1998), the extensional character, the soil conditions and the perseverance of the ground ruptures on any surface (either soil or construction; Fig. 8) imply that these are primary ruptures. Some scattered ruptures observed very near to the Titarissios river bank are most probably secondary ruptures due to ground shaking.

Taking into account the frequency and the size with which the ground effects appear, it is suggested that the earthquake belongs to degree VIII on the ESI-2007 scale (Michetti et al., 2007; Silva *et al.*, 2015).

6. SUMMARY AND DISCUSSION

The 2021 earthquake sequence in Tyrnavos-Elassona area revealed tectonic structures that were not concerned as active ones. Both focal mechanisms and the trend of the aftershock spatial distribution strongly suggest NW-SE-striking faulting. The focal mechanisms also revealed almost pure normal dip-slip kinematics and a NE-SW oriented extensional stress axis against the quasi-N-S one that was supposed to characterize the broader area of Thessaly. These geometry and kinematics are in agreement with the Quaternary faults that were discovered by a borehole network that was drilled during research on the lignite deposits in the Domeniko-Amourio sub-basin by Dimitriou and Giakoupis (1998). The NW-SE-striking fault mapped by IGME (1998) (Fig. 1) is considered as a south-eastern continuation of this fault system. Moreover, the spatiotemporal evolution of the sequence implies the rupture of two adjacent segments which produced the two strongest shocks, respectively.

The sequence was followed by several coseismic ground deformational phenomena, such as landslides/rockfalls, liquefaction and primary ruptures. The landslide and rockfalls were mostly associated with the ground shaking. The ruptures were observed west of the Titarissios River, near the Quaternary faults found by Dimitriou and Giakoupis (1998). Some of the ruptures were combined with extensive liquefaction phenomena. Others crossed reinforced concrete irrigation channels without changing their direction.

An emerging question is whether these ruptures represent (one of) the seismic faults that produced the strongest shocks. Although their direction fits the proposed nodal planes of the moment tensor solutions and the borehole findings, the hypocentral depths with the moderate-to-shallow dip angle, the InSAR images (Lekkas *et al.*, 2021) suggest that the rupture of the main seismic fault(s) emerged further to the south in the alpidic

bedrock, which is also supported by the observations of Chatzipetros *et al.* (2021, this volume). It is noteworthy to mention that Ferrière et al. (2004; 2011) has proposed the occurrence of a bounding detachment fault along the western margin of the Meso-Hellenic Trench, part of which is the broader study area, possibly facilitating the slip during a younger reactivation as an inherited structure. Possibly imitating the seismotectonic setting of the Corinth Gulf, where a deep low-angle detachment(?) fault branches into several parallel steeper faults towards the surface with simultaneous activity (Rigo *et al.*, 1996; Hatzfeld *et al.*, 2000), the recent sequence in Tyrnavos-Elassona area probably used two slip paths along two branches: the biggest amount of slip followed a southern branch, *i.e.* the prolongation of a deeper low-angle fault towards the surface, and a small amount possibly took a different path, through steeper faults, such as the ones discovered by Dimitriou and Giakoupis (1998), creating the systematic NW-SE-striking ground fissures of a 'secondary surface rupture' (term after DePolo *et al.*, 1991) and producing the extensive damages in the nearby constructions.

Fig. 9 (next page: Ground deformation phenomena observed in the epicentral area of the 2021 earthquake sequence. (a) Satellite image showing the ground deformation phenomena locations, the faults detected by Dimitriou and Giakoupis (1998; see also Fig. 3), and the neotectonic faults found in the literature (see Fig. 4 for references). (b, c) Ground ruptures with liquefaction. (d) Gneiss-schist boulder detachment in Domeniko village. (e) Rockfalls along the Tyrnavos-Elassona highway. (f) Ground rupture cutting through the asphalt road. (g, h) Rockfalls near the Panagia Olympiotissa Monastery (Elassona). Locations of all photographs are shown in (a).

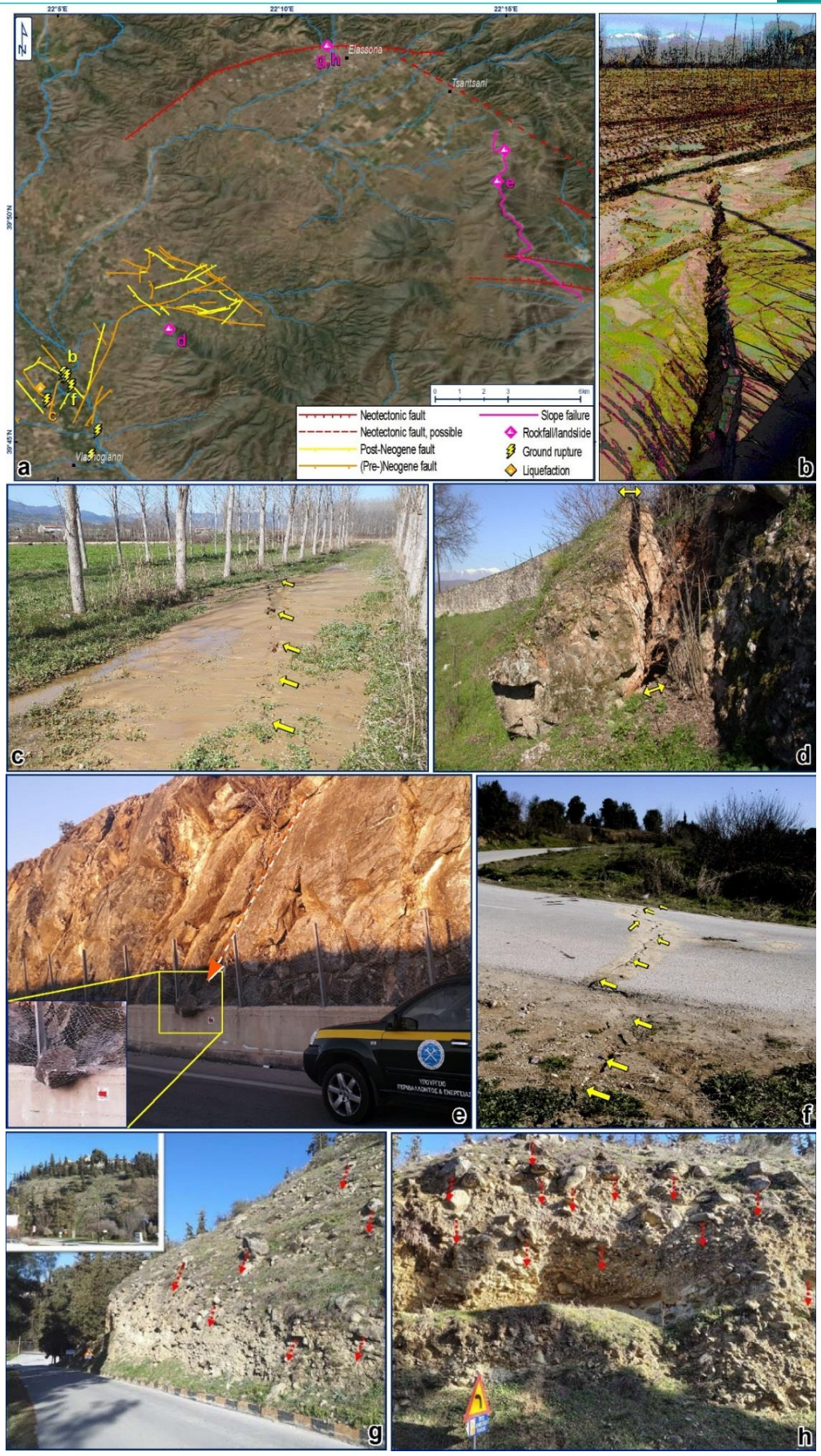
22°5'E
22°10'E
22°15'E
39°50'N
39°45'N
N
Elassona
Tsantsani
Vlachogianni
a
b
c
d
e
f
g
h
0 1 2 3 6km
Neotectonic fault
Neotectonic fault, possible
Post-Neogene fault
(Pre-)Neogene fault
Slope failure
Rockfall/landslide
Ground rupture
Liquefaction

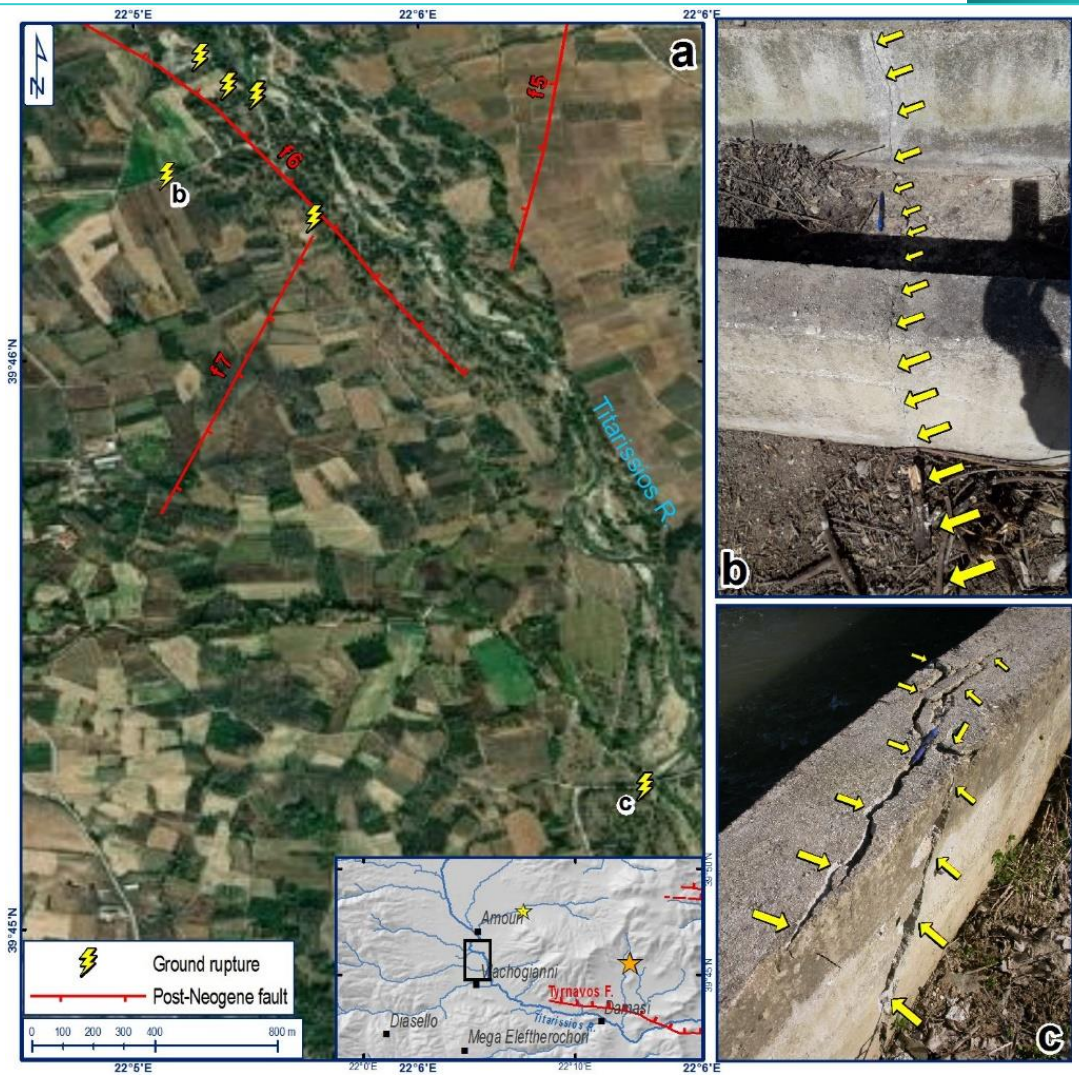

Fig. 10: Ruptures crossing irrigation channels. The construction of the channels is of reinforced concrete. The direction of the channels is (b) ENE-WSW (quasi-perpendicular to faulting), and (c) NNW-SSE (sub-parallel to faulting).

7. ACKNOWLEDGEMENTS

D.G. and S.S. would like to thank Prof. Emer. Sp. Pavlides for his insightful discussions. All authors also acknowledge the two reviewers who significantly improved the paper with their comments and suggestions.

8. REFERENCES

Caputo, R., 1993. Morphotectonics and kinematics along the Tirnavos Fault, northern Larissa Plain, mainland Greece. *Zeitsschrift für Geomorphol.*, 94, 167–185.

Caputo, R., Helly, B., 2005. Archaeological evidences of past earthquakes: a contribution to the SHA of Thessaly, Central Greece. *Journal of earthquake engineering*, 9(2), 199-222. doi: 10.1080/13632460509350539

Caputo, R., Pavlides, S. 1991. Neotectonics and structural evolution of Thessaly (Central Greece). *Bull. Geol. Soc. Greece*, 25, 119–133.

Caputo, R., Pavlides, S., 1993. Late Cainozoic geodynamic evolution of Thessaly and surroundings (central-northern Greece). *Tectonophysics*, 223, 339–362. doi: 10.1016/0040-1951(93)90144-9

Caputo, R., Chatzipetros, A., Pavlides, S., Sboras, S., 2012. The Greek database of seismogenic sources (GreDaSS): State-of-the-art for northern Greece. *Ann. Geophys*., 55, 859–894. doi: 10.4401/ag-5168

Chatzipetros, A., Pavlides, S., Foumelis, M., Sboras, S., Galanakis, D., Pikridas, C., Bitharis, S., Kremastas, E., Chatziioannou, A., Papaioannou, I., 2021. The northern Thessaly strong earthquakes of March 3 and 4 and their neotectonic setting. *Bull. Geol.Soc., Greece*, this volume.

DePolo, C.M., Clark, D.G., Slemmons, D.B. and Ramelli, A.R., 1991. Historical surface faulting in the Basin and Range province, western North America: implications for fault segmentation. *Journal of Structural Geology*, 13(2), 123-136. doi: 10.1016/0191-8141(91)90061-M

Dimitriou, D., Giakoupis, P., 1998. Mine research of coal deposit in Elassona: Domeniko sub-area. Technical report, Institute of Geological and Mineral Exploration (IGME), Athens [in Greek]

Earthquake Planning and Protection Organization – EPPO, 2000. Greek Antiseismic Regulation. EPPO, Athens.

Ferrière, J., Reynaud, J. Y., Pavlopoulos, A., Bonneau, M., Migiros, G., Chanier, F., Proust, J.N., Gardin, S., 2004. Geologic evolution and geodynamic controls of the Tertiary intramontane piggyback Meso-Hellenic basin, Greece. *Bulletin de la Société géologique de France*, 175(4), 361-381. doi: 10.2113/175.4.361

Ferriere, J., Chanier, F., Reynaud, J. Y., Pavlopoulos, A., Ditbanjong, P., Migiros, G., Coutand, I., Stais, A., Bailleul, J., 2011. Tectonic control of the Meteora conglomeratic formations (Mesohellenic basin, Greece). *Bulletin de la Société Géologique de France*, 182(5), 437-450. doi: 10.2113/gssgfbull.182.5.437

Galanakis, D., 1997. *Neotectonic structure and stratigraphy Neogene and Quaternary sediments of Almyros-Pagasitikos basin, Pilio, Oreoi-Trikeri strait and Maliakos Gulf*. PhD Thesis, Aristot. Univer. Thessaloniki, Unpub., 260 p.

Galanakis, D., Pavlides, S., Mountrakis, D., 1998. Recent Brittle Tectonic in Almyros -Pagasitikos, Maliakos, N. Euboia and Pilio. *Bull. Geol. Society of Greece*, 32(1), 263-273.

Giardini, D., Wössner, J., Danciu, L., 2014. Mapping Europe's seismic hazard. *Eos, Transactions American Geophysical Union*, 95(29), 261-262. doi: 10.1002/2014EO290001

Hatzfeld, D., Karakostas, V., Ziazia, M., Kassaras, I., Papadimitriou, E., Makropoulos, K., Voulgaris, N., Papaioannou, C., 2000. Microseismicity and faulting geometry in the Gulf of Corinth (Greece). *Geophysical Journal International*, 141(2), 438-456. doi: 10.1046/j.1365-246x.2000.00092.x

IGME – Institute of Geology and Mineral Exploration, 1987. Geological Map of Greece, "Elasson" sheet, 1:50.000 scale, IGME, Athens

IGME – Institute of Geology and Mineral Exploration, 1998. Geological Map of Greece, "Farkadon" sheet, 1:50.000 scale, IGME, Athens

ITSAK–DUTh, 2021. Thessaly Earthquakes M6.3, 03/03/2021 and M6.1, 04/03/2021. Preliminary Report. Research Unit ITSAK, EPPO and Department of Civil Engineering, DUTh. Thessaloniki. pp. 63. doi: 10.5281/zenodo.4641200

Kiratzi, A., Louvari, E., 2003. Focal mechanisms of shallow earthquakes in the Aegean Sea and the surrounding lands determined by waveform modelling: A new database. *J. Geodyn*., 36, 251–274. doi: 10.1016/S0264-3707(03)00050-4

Lekkas, E., Agorastos, K., Mavroulis, S., Kranis, C., Skourtsos, E., Carydis, P., Gogou, M., Katsetsiadou, K.-N., Papadopoulos, G., Triantafyllou, I., Agalos, A., Moraitis, S.,

Stamati, E., Psarris, D., Kaviris, G., Kapetanidis, V., Papadimitriou, P., Karakonstantis, A., Spingos, I., Kouskouna, V., Kassaras, I., Pavlou, K., Voulgaris, N., Mavrouli, M., Pavlides, S., Chatzipetros, A., Sboras, S., Kremastas, E., Chatziioannou, A., Kiratzi, A., Papazachos, C., Chatzis, N., Karakostas, V., Papadimitriou, E., Koukouvelas, I., Nikolakopoulos, K., Kyriou, A., Apostolopoulos, D., Zygouri, V., Verroios, S., Belesis, A., Tsentzos, I., Krassakis, P., Lymperopoulos, K., Karavias, A., Bafi, D., Gatsios, T., Karatzia, M., Gkougkoustamos, I., Falaras, T., Parcharidis, I., Papathanassiou, G., Evangelidis, C.P., Karastathis, V., Tselentis, G-A., Ganas, A., Tsironi, V., Karasante, I., Valkaniotis, S., Galanakis, D., Kostantopoulou, G., Papadopoulos, N., Kourou, A., Manousaki, M., Thoma, T., 2021. The early March 2021 Thessaly earthquake sequence. *Newsletter of Environmental, Disaster and Crises Management Strategies*, 22, ISSN 2653-9454.

Michetti, A.M., Esposito, E., Guerrieri, L., Porfido, S., Serva, L., Tatevossian, R., Vittori, E., Audemard, F., Azuma, T., Clague, J., Comerci, V., 2007. Intensity scale ESI 2007 (La scala di Intensità ESI 2007). In: Guerrieri, L., Vittori, E. (Eds), *Memorie Descrittive della Carta Geologica d'Italia, 74, Servizio Geologico d'Italia, Dipartimento Difesa del Suolo, APAT, Rome*, pp. 41

Papazachos, B., Papazachou, K., 2003. Earthquakes of Greece. Ziti editions, Thessaloniki.

Perissoratis, C., Angelopoulos, I., Mitropoulos, D., 1991. Surficial Sediment Map of the Aegean Sea Floor, 1:200 000 scale, "Pagasitikos" Sheet, IGME, Athens.

Rigo, A., Lyon-Caen, H., Armijo, R., Deschamps, A., Hatzfeld, D., Makropoulos, K., Papadimitriou, P., Kassaras, I., 1996. A microseismic study in the western part of the Gulf of Corinth (Greece): implications for large-scale normal faulting mechanisms. *Geophys. J. Int*., 126(3), 663-688. doi: 10.1111/j.1365-246X.1996.tb04697.x

Sboras, S., 2011. *The Greek Database of Seismogenic Sources: seismotectonic implications for North Greece*. Pubblicazioni dello IUSS, 5(1), PhD thesis, Università degli Studi di Ferrara, pp. 252.

Silva, P. G., Guerrieri, L., Michetti, A. M., 2015. Intensity scale ESI 2007 for assessing earthquake intensities. In: Beer, M. et al. (Eds), *Encyclopedia of Earthquake Engineering*, Springer-Verlag, 1219-1237.

Tadono, T., Ishida, H., Oda, F., Naito, S., Minakawa, K., Iwamoto, H., 2014. Precise global DEM generation by ALOS PRISM. ISPRS Annals of the Photogrammetry, *Remote Sensing and Spatial Information Sciences*, 2(4), 71. doi:10.5194/isprsannals-II-4-71-2014

Woessner, J., Laurentiu, D., Giardini, D., Crowley, H., Cotton, F., Grünthal, G., Valensise, G., Arvidsson, R., Basili, R., Demircioglu, M.B., Stucchi, M., 2015. The 2013 European seismic hazard model: key components and results. *Bulletin of Earthquake Engineering*, 13(12), 3553-3596. doi: 10.1007/s10518-015-9795-1